

**A**  
**Thesis Report**  
**on**  
**“ENERGY SCAVENGING USING MEMS BASED POWER GENERATOR”**

Submitted towards the fulfillment of requirement for the award of degree of

**Master of Engineering**  
**In**  
**Electronics and Communication Engineering**

**Submitted by:**

Rajat Kant

Roll No: 801361021

**Under the Guidance of:**

Dr. Anil Arora

Assistant Professor

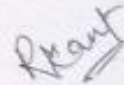


**ELECTRONICS AND COMMUNICATION ENGINEERING DEPARTMENT**  
**THAPAR UNIVERSITY**  
(Established under the section 3 of UGC Act, 1956)  
**PATIALA – 147004 (PUNJAB)**

## DECLARATION

I hereby declare that the thesis report entitled "ENERGY SCAVENGING USING MEMS BASED POWER GENERATOR" is an authentic record of my study carried out as requirement for the award of degree of ME (Electronics and Communication Engineering) at Thapar University, Patiala, under the supervision of Dr. Anil Arora (Assistant Professor), "Electronics and Communication Engineering Department" during 4<sup>th</sup> semester, 2015

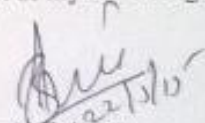
Date: 21-05-2015



Rajat Kant  
Roll No-801361021

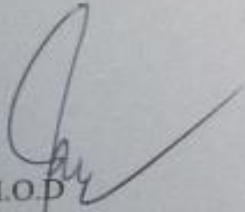
It is certified that the above statement made by the student is correct to the best of my knowledge and belief.

Date:

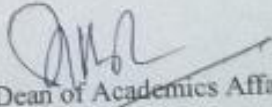


Dr. Anil Arora  
Assistant Professor  
ECED

Countersigned by



H.O.D.  
ECED, Thapar University,  
Patiala, 147004



Dean of Academics Affairs  
Thapar University,  
Patiala, 147004

## **ACKNOWLEDGEMENT**

I would like to express my gratitude to Dr. Anil Arora, Assistant Professor, electronics and communication engineering department, Thapar University, Patiala for his patience, guidance and support throughout this report work. I am truly very fortunate to have the opportunity to work with him. He has provided help in technical writing, presentation style and I found this guidance to be extremely valuable.

I am also thankful to entire faculty, staff members and H.O.D of Electronics & Communication Engineering Department for their encouragement.

I am greatly indebted to all my friends, who have graciously applied themselves to the task of helping me with ample moral support and valuable suggestion. Finally, I would like to extend my gratitude to all those persons who directly or indirectly helped me in process and contributed toward this work.

**Rajat kant**

**801361021**

# TABLE OF CONTENTS

<b>Declaration</b>	(ii)
<b>Acknowledgement</b>	(iii)
<b>Table of contents</b>	(iv)
<b>List of figures</b>	(vii)
<b>List of tables</b>	(vii)
<b>Abstract</b>	(ix)
<b>CHAPTER 1- Introduction</b>	1
1.1 Power mems	1
1.2 Research motivation	1
1.3 Objective of thesis	2
1.4 Thesis outline	3
<b>CHAPTER 2- Literature review and background</b>	5
2.1 Introduction	5
2.2 Overview of the existing power sources for MEMS	5
2.2.1 Solar energy conversion .	5
2.2.2 Thermal energy conversion	6
2.2.3 Vibrational energy conversion	6
2.2.4 Human body energy	7
2.3 Vibration to electricity conversion generators	7
2.3.1 Piezoelectric generators	7
2.3.2 Electrostatic generators	8
2.3.3 Electromagnetic Generators	8
2.4 Classification of electromagnetic microgenerators and comparison	14
2.5 Compact suspension system	17

2.6 Spring design objectives and considerations	19
2.7 Magnetic circuit	20
2.7.1 Permanent magnet	20
2.8 Coil configuration design	22
2.9 Summary	23
<b>CHAPTER 3- Analysis of Electromagnetic Microgenerator Design</b>	<b>25</b>
3.1 Introduction	25
3.2 Analytical model proposed	26
3.3 General principle of operation	28
3.4 Summary	29
<b>CHAPTER 4- Modelling and Simulation</b>	<b>30</b>
4.1 Introduction	30
4.2 Theoretical considerations of the suspension design	30
4.2.1 Static considerations	30
4.2.1.1 Stress and strain	31
4.2.1.2 Deflection of the flat spring	31
4.2.2 Dynamic considerations	32
4.2.2.1 Vibration of a spring mass system	32
4.2.3 Material selection	33
4.3 Finite-Element Modelling	33
4.3.1 Suspension model simulations	35
4.4 FEA to calculate the magnet-coil separation	38

4.5 Simulated voltage	39
4.6 Summary	41
<b>CHAPTER 5- Conclusion</b>	42
5.1 Comparison study of the electromagnetic microgenerator	42
5.2 Suggestions for Future Work	43

## LIST OF FIGURES

Fig.2.1 Design of beam-mass structures.	17
Fig.2.2 Different suspension structures.	18
Fig.2.3 BH loop.	21
Fig.2.4 Coil types in MEMS, a) Multilayer wire microcoils. b) Idealized solenoidal coil geometry. c) Idealized multilayer coil geometry. d) photograph showing top layer of a stator coil.	22
Fig 3.1 Schematic of an electromagnetic generator .	26
Fig. 3.2 Simplified equivalent circuit model of electromagnetic microgenerator.	28
Fig.4.1 Cantilever beam in the original position.	30
Fig. 4.2 Basic diagram of the deflection of cantilever beam with concentrated force $F$ applied at the free end of the beam and Moment $M$ applied at the free end of the beam.	31
Fig.4.3 Spring mass system with single degree of freedom .	32
Fig.4.4 COMSOL finite element models for the Suspension designs, a)1 beam(cantilever), b) 2 beam , c)spring beam and d)multiple beam	35
Fig. 4.5 The magnetic induction field $B$ at a distance $200\mu\text{m}$ .	38
Fig.4.6 COMSOL results of average $B$ versus distance between the coil and the magnet.	39
Fig. 4.7 output voltage $v/s$ a) no. of turns b) magnetic field c) frequency.	41

## LIST OF TABLES

Table 2.1 Comparison of performance of various electromagnetic microgenerators.	15
Table 2.2 Comparison of performance of various electromagnetic microgenerators(cont.)	16
Table 4.1 Properties of materials considered for the mechanical spring.	33
Table 4.2 Results of maximum deflection in z- direction.	36
Table 4.3 a) deflections for different beam lengths.	37
Table 4.3 b) deflections for different beam widths.	37
Table 5.1 Comparison between the reported electromagnetic generators based on moving magnet.	43

## ABSTRACT

Over the past few years, there has been a huge reduction in size and power consumption of MEMS devices like transducers and sensors. These devices are usually designed to run on batteries the replacement of batteries is not practical. The limited lifespan of batteries may induce costly maintenance, in the case of contaminated areas for instance. Moreover, batteries dying without warning cause serious problems in safety monitoring applications. That led to a surge of research in the area of energy harvesting. Sustainable power generation may be achieved in converting ambient energy into electrical energy. Some possible ambient energy sources are, for instance, thermal energy, light energy and mechanical energy. After an extensive survey of potential energy harvesting methods, the conversion of ambient vibrations to electricity was chosen as a method for further research. Since mechanical vibrations exist in most systems, many works focused on vibration-driven generators. In this field, the electromagnetic induction is well suited for the mechanical to electrical energy conversion. The design of the mechanical system that transmits the surrounding vibratory energy to the electromagnetic generator is a critical importance.

This thesis presents an optimization of an electromagnetic microgenerator. It describes the theory, design and simulation of an energy converter based on electromagnetic induction. The objectives of this research are designing, improving the performance and operational reliability of electromagnetic microgenerator. These have been achieved by identifying the desirable design features of the electromagnetic microgenerator. Extensive analytical investigation has been conducted to develop an efficient design of an electromagnetic microgenerator. This thesis deals with the design and simulation of a number of suspension structures to be used for supporting the moving magnet of an electromagnetic microgenerator. These suspension structures were designed by modeling and finite element method simulation using COMSOL Multiphysics. This helped in understanding the critical aspects of the design at the same time leading to the determination of the optimum parameters for the structures, such as static deflection.

# CHAPTER-1

## INTRODUCTION

### 1.1 Power MEMS

The advancements in fabrication and micromachining techniques have accelerated the functionality of MEMS devices, which is one of the important reasons for the emergence of sustainable power sources. Power MEMS is the newest category of MEMS, which encompasses micro devices and microsystems for power generation and energy conversion. The research and development of power MEMS have been promoted by the need for compact power sources with high energy and power density. Power MEMS has expanded to include not only various MEMS based power generators but also small energy machines and micro devices for macro power generators. As various devices and systems, such as energy harvesting micro devices are presented in the literature. Their power levels have a variation from ten nanowatts to ten of microwatts.

### 1.2 Research Motivation

In the past few years the need for developing self-powered wireless sensing systems has increased. Wireless sensor networks are made of large numbers of small, low-cost sensor nodes working in collaboration to collect data and transmit them to a base station via a wireless network. Wireless sensing systems could extensively be used for a wide variety of applications. Powering remote sensing systems becomes a problem due to the difficulty of battery replacement and the cost of wiring power to them. Therefore, many researchers focused on energy harvesting from the environment. In the field of MEMS power generation, electromagnetic, piezoelectric and electrostatic generators have been developed.

Vibrational energy scavenging has found application in distributed wireless applications [1], and has been proposed as a third major renewable energy source available to a mobile computing platform after photovoltaic and thermoelectric sources [2]. Researchers have so far worked on harvesting energy from environmental sources like solar, thermal, wind, and vibrations to power up these devices. Among these techniques, vibrations seem to be more attractive due to their availability, high power density, and easiness of integration to micro fabrication and assembly. So far, mainly three types of vibration based techniques have been

utilized to harvest energy: capacitive, piezoelectric, and electromagnetic. We are here focused on using the principle of electromagnetic induction for the generation of electrical power from low frequency vibrations in the environment. However, the ambient vibrations exist in the low frequency range which did not result in significant amount of power, in the past it was 0.25 nano Watts in first generation MEMS devices. For this reason, the main objective is to propose a new design that can be able to generate good amount of energy even in the ambient range.

### **1.3 Objectives of the thesis**

The aim of this research is to investigate the methodology for designing and fabricating electromagnetic micropower generating devices at microlevel. Such micro generating device can be used to power wireless sensors network in remote or difficult to access applications.

This research consists of:

- Reviewing the literature about power generation for MEMS with particular emphasize on the principles of electromagnetic conversion devices at micro level.
- Describing the design of a new electromagnetic micropower generating device. This has been made possible by: (1) investigating and optimizing the mechanical and electrical properties of the materials employed. These properties have a direct effect on each part of the design. For example in the case of a spring design, material type and its properties limit the spring displacement which is needed to be as large as possible within the device volume, (2) Selecting patterns for each component in the design . The spring pattern should be selected with low damping ratio, and (3) Using standard simulation software COMSOL to build the design.
- Developing an analytical model to carry an investigation for the optimum microgenerator design parameters.
- Developing an analytical finite element models for mechanical and magnetic characterization to optimize (comparison of a few flat spring designs and selecting the best) the proposed electromagnetic microgenerator.

## **1.4 Thesis outline**

**Chapter 2**, reviews the literature on the existing power sources particular for MEMS devices, with the focus on electromagnetic induction. Detailed descriptions of the ongoing research on electromagnetic microgenerators are given. The electromagnetic microgenerators that have been reported in the literature are broadly classified as the moving magnet, the moving coil type and or the spring type. A general vibration to electricity model, provided by Williams and Yates (Williams and Yates 1995), is presented and discussed. The major steps to improve the electromagnetic microgenerator are presented. Designs of the compact suspension system are presented. The design objectives and specifications of the flat spring to be used in the electromagnetic micro generator are discussed. A brief literature about the permanent magnet material selection and the coil configuration are given.

**Chapter 3** also presents an extensive analytical investigation to develop an efficient design of an electromagnetic microgenerator. A number of issues associated with the design of the microgenerator are addressed. A description of the basic operating principles of the electromagnetic microgenerator is presented. An analytical model is used for parametric study, optimization and reliability analysis of the microgenerator.

**Chapter 4** provides details of the magnetic analyses performed on the proposed electromagnetic microgenerator. The objectives behind this are to characterize the permanent magnet and to investigate the optimum position of the coil relative to the magnet. An analytical model of the coil is reviewed. The coil dimensions are set according to the analytical model to be used for the magnetic analyses. The results were obtained using the finite element package COMSOL 2D for static magnetic simulation. Finite element model is developed for the electromagnetic microgenerator. Initially finite element analyses (FEA) of

the permanent magnet and the coil are undertaken separately.

**Chapter 5** summarizes the research outcomes. Useful conclusions drawn from the work carried out in this thesis are discussed and directions for future research are suggested

## CHAPTER 2

### LITERATURE REVIEW AND BACKGROUND

#### 2.1 Introduction

In this chapter, a review of the literature on the existing power sources that are applicable to MEMS devices is given. The basic fundamentals of operation and the efficiency of the devices that convert the ambient energy to electricity are reviewed. Vibrations to electricity conversion devices are presented. Detailed descriptions of the ongoing research on electromagnetic microgenerator are given. The operating principles, the advantages and disadvantage of the various electromagnetic microgenerator designs that have been reported in the literature are discussed through a comparative study. A general model of the electromagnetic microgenerator is presented. A brief background about the history of the flat spring is given and a discussion the spring design objectives and considerations to be used in the electromagnetic microgenerator is provided. These points are important to help with the design. A brief literature about the design of the permanent magnet and the coil configuration is given.

#### 2.2 Overview of the existing power sources for MEMS

Most MEMS devices generally utilize macroscopic power sources and they greatly limit the main advantage of size reduction of MEMS devices. Batteries are commonly used for powering MEMS, however, they exhibit shorter lifetime, less power storage and large weight and volume in comparison with the device they power. Also chemicals contained in the batteries may be toxic. Moreover, in some applications the battery replacement is an expensive and difficult process or may be inconvenient for devices that are implanted in human patients like medical sensors. Therefore, spectacular efforts have been made by researchers to find alternative power supplies to cover the drawbacks of using batteries in MEMS applications. Some of these supplies can be specially designed to convert the ambient energy in the environment into electrical power.

##### 2.2.1 Solar energy conversion

An abundant source of ambient energy is solar energy. A solar cell is a device that produces electrical energy directly from solar radiation. The solar radiations have the power density of

about  $1.4 \text{ kw/m}^2$  and it changes slightly by 0.1% during the year [3]. The basic device requirements of a solar cell are an electronic asymmetry, such as a p-n junction. When illuminated, electron-hole pairs are generated throughout the solar cell. If the cell is connected to a load, current will flow from one region of the cell, through the load, and back to the other region of the cell. Solar self powered devices such as calculator and watches are common place. Lee et al. [4] developed a thin solar cell that is specifically designed to produce the open circuit voltages which is required to supply MEMS electrostatic actuators. The array consists of 100 single solar cells connected in series, occupying a total area of only  $1\text{cm}^2$ . Connecting the array to micro-mirror, a microsystem is produced that respond to the modulation of the applied light.

The efficiency of the solar cell varies depending on their usage in outdoor to indoor environments, where the light intensity is different and the differences of the incident light angle in both conditions. The efficiency is about 10-20 % and it depends on the silicon crystal type. A typical single crystal silicon PV cell having an area of  $100 \text{ cm}^2$  could produce approximately 1.5 watts of power at 0.5 volts DC and 3 amps under full summer sunlight. The power output of the cell is directly proportional to the intensity of the sunlight. This type of power generation is limited to the applications with access to light.

### **2.2.2 Thermal energy conversion**

Temperature differences can also provide an ambient energy exploited to generate power. Thermoelectric generators are devices used to convert thermal energy directly to electrical energy. Such devices are based on thermoelectric effects involving interactions between the flow of heat and of electricity through solid bodies. A typical thermoelectric module has an array of semiconductor pellets that have been doped so that one type of charge carrier either positive or negative carries the majority of current. The pairs of P-N pellets are configured in such a way that they should be connected electrically in series, but thermally in parallel. When a temperature gradient is created across the thermoelectric device, a DC voltage develops across the terminals. When a load is properly connected, electrical current flows through the device.

### **2.2.3 Vibration energy conversion**

The low amplitude vibrations present in the environment has an associated mechanical energy with them, is another source of ambient energy that can be converted into electrical energy. The low amplitude ambient vibrations are present in our surrounding structures like bridges, tall structures, vehicles etc. The main design prospective of the vibration generators is to use the ambient vibrations into the movement and then to use that movement of the suspension mass into electrical energy by electromagnetic induction.

### **2.2.4 Human body energy**

In human body, the various kinds of energy like breathing, walking, finger movement can be feasibly extracted and converted into electrical energy. Starner, and Shenck et.al. [5] had a research on scavenging the energy which is used passively and wasted by the human body. They found that maximum energy obtained through walking which is about 6-8 watts. This research leads to the development of piezoelectric shoe inserts but the only problem is how to get the energy from the shoe and give it to the other places of the body.

## **2.3 Vibration to electricity conversion generators**

### **2.3.1 Piezoelectric generators**

A technique for generating power from vibration was presented by Glynne-jones et.al. and White et.al [6]. A device is developed from a thick-film piezoelectric layer (piezoceramic lead zirconate titanate, PZT) deposited on to a very thin steel beam. As the beam oscillates, the piezoelectric layer begins to deform. This deformation causes the production of charge across electrodes positioned on the top and bottom surfaces of the piezoelectric element. The resulting potential difference can be utilized to produce electrical energy. The device is designed keeping in mind that it should have simplified design rather than optimal design for electrical power.

An optimal design for piezoelectric generator was published by Ottman et.al. [7]. The focus their work on the optimal design of the generator conditioning electronics for a piezoelectric generator driven by vibration. The circuit consists of an ac-dc rectifier, output capacitor, an electrochemical battery, and a switchmode dc-dc converter that helps in controlling the energy

flow into the battery. The maximum power output reported is 18 mw. The size of the piezoelectric converter is  $19\text{cm}^2$  at a driving vibration of 53.8 Hz.

The piezoelectric generators can directly convert the ambient vibrations into a voltage output by using an electroded piezoelectric material. There is no requirement for having complex geometries but the piezoelectric materials are required to be strained directly and therefore their mechanical properties will limit the overall performance and lifetime. The disadvantage of piezoelectric conversion is their problem of implementation on the microscale and integration with microelectronics.

### **2.3.2 Electrostatic generators**

The electrostatic generator designed by Meninger et.al. and Roundy et.al. [8] utilizes ambient mechanical vibration and convert them into electrical energy by using MEMS variable capacitor. By placing charge on the capacitor plates, the voltage will increase as the capacitance decreases and vice versa. If the voltage is placed on the capacitor, charge will move from the capacitor as the capacitance decreases. In both cases, mechanical energy is converted into electrical energy which can be stored and utilized by a load. The major problem associated with capacitive converters is that some method must be employed to hold the voltage, across the MEMS device, constant during the conversion process, which requires a separate voltage source. It is also not capable of converting sufficient power per unit volume. The maximum predicted output power from electrostatic generator is  $8\ \mu\text{W}$ . Parasitic capacitances within the structure can sometimes lead to reduced generator efficiency and there is risk of capacitor electrodes shorting or of ‘stiction’ in wafer-scale implementations.

### **2.3.3 Electromagnetic Generators**

Amarithajah and Chandrakasan et. al. in 2000 designed a generator in a macro size and designed to work from vibrations induced by human walking, and is predicted to produce  $400\ \mu\text{W}$  of power from 2cm movement at frequency of 2Hz. The generator that consists of a wire coil  $l$  attached to a mass  $m$  connected to a spring  $k$ . The other end of the spring is attached to a rigid housing. A permanent magnet  $B$  is attached to the housing. As the housing is vibrated, the mass moves relative to the housing and energy is stored in the mass spring system. The moving coil through the field of a permanent magnet cuts the varying amount of magnetic

flux, which in turn induces a voltage on the coil according to Faraday's Law of induction. Their simulation and measured result of the output voltage showed significant differences. The device was designed to have maximum power of 400  $\mu\text{W}$  under ideal conditions without mechanical losses. The vibration source was 2cm and 2Hz to estimate the human walking for their model. As they reported the measured output voltage which was 180mV, they did not report the output power. However, 180mV was still too small for their application and they needed a transformer to rectify the voltage and this one can vary both the electrical and mechanical parameters [9].

El-hami et.al. in 2001 presented a generator consisting of a magnetic core mounted at the tip of a planar steel beam. The design utilizes an electromagnetic transducer and its operating principal is based on the relative movement of a magnet pole with respect to a coil. As the device is vibrated, the resonant beam oscillates back and forth, moving past a coil of a few turns. The results show an output power of 0.53mW with an input vibration of amplitude 25  $\mu\text{m}$ , and frequency 322Hz. Excluding the clamp at the base of the beam and the coil mounting, the device requires a volume of 0.24 $\text{cm}^3$ . It is clearly shown that device size is not in micro level and micromachining techniques were not used in its construction [10].

Ching et.al in 2002 has developed a generator similar to the preposed generator by Li et. al. in 2000. It is micromachined generator that comprises a permanent magnet mounted on a laser-micromachined spiral spring structure next to PCB coil. A laser system was used to micromachined the resonating copper springs. The spring is designed to let the mass vibrate horizontally while the input vibration is applied vertically, and that this horizontal vibration increases the output voltage of the generator. This can be explained by faraday's law of induction which stated that the voltage output should be proportional to the rate of changing magnetic flux. The generator have an improved spiral spring resulted on a peak to peak output voltage of up to 4.4V and a maximum power of 830 $\mu\text{w}$  when driven by 200 $\mu\text{m}$  displacement at its resonant frequency of 110Hz. The generator total volume is 1 $\text{cm}^3$  [11].

Kulah and Najafi in 2004 describe a silicon-based generator, which comprises two separate chips combined together. Their device utilizes two resonant structures that are designed to

achieve mechanical up-frequency conversion. The authors argue that because most silicon structures have relatively high resonant frequencies (several kHz) and a majority of ambient vibration frequencies are less 100 Hz, then a device that can perform mechanical upfrequency conversion will provide an efficient solution to energy harvesting problems. To demonstrate this, they have fabricated a silicon generator that has an upper diaphragm with a resonant frequency of 25 Hz. An NdFeB magnet on the upper diaphragm is used to excite a lower structure into resonance through magnetic attraction. The lower diaphragm has a resonant frequency of around 11 kHz. Integrated coils are fabricated on the lower structure. The author quote the theoretical maximum power generated as being  $2.5 \mu\text{W}$ , but they only measured  $4\text{nW}$  from a millimetre-scale device. The level of input mechanical excitation is not quoted in the paper [1].

Glynne-jones et. al. in 2004 present experimental results obtained from prototypes fabricated using batch micromachining and hand assembly with different magnet configurations. They followed the work of El-hami et.al. in 2001 [10]. The initial prototype was based on moving magnets and had an overall volume of  $0.83\text{cm}^3$ . The second device was a moving four-magnet generator (with a fixed coil), having an overall volume of  $3.15 \text{ cm}^3$ . The first prototype generated power levels up to  $180 \mu\text{W}$ , for a free end beam displacement of  $0.85\text{mm}$ . The second prototype was aimed at improving the magnitude of the output voltage by improving the magnetic coupling between the magnets and coil. For the same input vibration, the second generator produced more than twice the output voltage and four times the instantaneous power. The authors present the results showing the response from a generator mounted on the engine block of a car. An instantaneous power of  $4\text{nW}$  was measured during a journey of  $1.24 \text{ Km}$  and the average power found to be  $157 \mu\text{W}$  [12].

Koukharenko et.al. in 2006 present a silicon microgenerator. The generator consists of a cantilever paddle, four magnets and a coil. The coil is recessed in a silicon cantilevered paddle designed to vibrate laterally in the plane of the wafer. Discrete magnets are positioned within etched recesses in capping wafers that are bonded to each face of the middle wafer. Three sets of supporting paddle beam dimensions have been simulated, each  $1 \text{ mm}$  long and  $500 \mu\text{m}$  thick. In model A the beam is  $500 \mu\text{m}$  wide, model B  $400 \mu\text{m}$  wide and C  $300 \mu\text{m}$  wide. The

resonance frequencies for the beams were 9.812, 7.149, 4.743 respectively, and the output power was found to be 2, 1.45, and 0.96 accordingly. The coil used in the initial simulation is a conventionally wound enameled copper coil with 600 turns of 25  $\mu\text{m}$  wire. The outer diameter of the coil is 2.4 mm and the inner diameter is 0.6 mm. The separation between magnets and coil is 0.1 mm. The resulting mass of the silicon paddle plus coil is measured to be  $2.8 \times 10^{-5} \text{Kg}$ . The magnets used were sintered NdFeB with dimensions of  $1 \times 1 \times 3 \text{ mm}$ . The results from a model A cantilever generator with a beam width of 500  $\mu\text{m}$ . This was found to have a resonant frequency of 9.5 kHz and generated 122 nW [13].

Another electromagnetic microgenerator has been proposed by Pan et.al. in 2006. They fabricate and analyse an electromagnetic microgenerator using MEMS technology. The generator consists of a FePt permanent magnet sputtered on a silicon membrane and Cu planar coil. The spring pattern is 100 $\mu\text{m}$  in width, 40  $\mu\text{m}$  in thickness and 100  $\mu\text{m}$  in gap. The dimensions of the coil have the thickness of 15  $\mu\text{m}$ , line width of 30  $\mu\text{m}$  and 50 turns. Maximum power was 100 and voltage of 40mv at a resonance frequency of 60Hz [14].

Wang et. al. in 2007 presents an electromagnetic micro power generator fabricated using microelectromechanical systems technology. The microgenerator consists of a permanent magnet of NdFeB, a copper planar spring and a two-layer copper coil. The structure is composed of an upper resonant structure on silicon wafer and a lower two-layer copper coil on glass substrate. The resonant structure is a vertically polarized NdFeB permanent magnet attached to the centre of a copper planar spring which consists of four spring beams and a platform. When the magnet is vibrating, it will move towards the coil and cause the change of the magnetic flux in the coil. The generator can generate 60mV ac peak–peak with an input frequency of 121.25Hz and at input acceleration of  $14.7 \text{m/s}^2$  [15].

Serre et. al. in 2008 present a design of an electromagnetic microgenerator by using a moving magnet on a polyimide film and a fixed planar coil made of aluminium layer. A generator prototype has been fabricated with a modular manufacturing process in which the coil, the magnet and the polyimide film are manufactured separately, diced and then assembled. The device produced a power of 200nw at a resonant frequency of 360Hz for a displacement of 6.8 $\mu\text{m}$  [16].

Saha et.al. develop a generator consist of axially magnetized permanent magnets placed vertically inside a tube so that facing surfaces have the same polarization. Thus the magnets repel one another. Two magnets are fixed at both ends of the generator tube housing. The middle is free to move but is suspended between fixed end magnets in the generator housing due to the repulsive force. A coil is wrapped around the outside of the tube. When the tube is vibrated the middle magnet vibrates up and down, and a voltage will be induced in the coil. There is no mechanical beam in this generator and suspended moving magnet works as magnetic spring constant. The generator millimeter prototype consists of two opposite polarity circular magnets tightly glued to a 3mm thick magnetic pole piece. This combination was inserted into a hollow Teflon tube so that it can move freely. After inserting, the two opposite polarity magnets were fixed on the both ends of the Teflon tube and 40 $\mu$ m copper wire with 1000 turns coil was wrapped around the tube at a point midway between the ends of the tube. The prototype generators generated 0.3–2.46mW when placed inside a rucksack which was worn during walking and slow running [17].

Sari et.al. present a generator covering a wide band of external vibration frequency by implementing serially connected parylene cantilevers in different lengths resulting in an array of cantilevers with varying natural frequencies. The simulation results showed that by utilizing 40 cantilevers and a length increment of 3 $\mu$ m, a frequency band of 1 KHz could be covered with a maximum steady power output of 0.4 $\mu$ w and a maximum voltage output of 50mV. The tests show that by utilizing 35 cantilevers, the fabricated device generates 10mV voltage and 0.4  $\mu$ w power continuously within a frequency band of 800Hz [18].

Kulkarni et. al. present three different designs of power generators which are partially micro-fabricated and assembled. Prototype A having a wire-wound copper coil, Prototype B, an electrodeposited copper coil both on a deep reactive ion etched (DRIE) silicon beam and paddle. Both devices have a volume of 106mm<sup>3</sup>. Prototype C uses moving NdFeB magnets in between two micro-fabricated coils. The integrated coil, paddle and beam were fabricated using standard micro-electro-mechanical systems (MEMS) processing techniques. The device volume was 150mm<sup>3</sup>. For Prototype A, the maximum measured power output was 148nW at

8.08 kHz resonant frequency and 3.9 m/s<sup>2</sup> acceleration. For Prototype B, the microgenerator gave a maximum load power of 23nW for an acceleration of 9.8 m/s<sup>2</sup>, at a resonant frequency of 9.83 kHz. Prototype C generates a maximum load power of 586nW across 110Ω load at 60 Hz for an acceleration of 8.829 m/s<sup>2</sup> [19].

In 2010, Turkeyilmaz S., Kulah H., Muhtaroglu A., proposed another design in which cantilevers are replaced by diaphragm. The cantilevers initially used causing phase shift. By using diaphragm, the scaling problem is reduced and the output of 119 nW was obtained [20].

In 2011, S. Turkilmaz and O.Zorlu from Department of Electrical and Electronics Engineering, Middle East Technical University, Ankara, Turkey presents an electromagnetic (EM) micro-power generator with tunable resonance frequency which can harvest energy from low frequency environmental vibrations. The reported power generator up-converts low frequency environmental vibrations before mechanical-to-electrical energy conversion by utilizing two diaphragms with different resonance frequencies. Power is generated through electromagnetic induction by a magnet attached to the low frequency diaphragm, and a 50 turn, 2.1 Ω coil, and a magnetic piece on the high frequency diaphragm. Both of the diaphragms are fixed to a common frame via rubber springs, which makes the resonance frequency of each diaphragm tunable. The fabricated prototype generates 5.2 mV and 3.21μW RMS power by up-converting 13 Hz, 7.5 mm peak-to-peak vibrations to 200 Hz. Tunability of the resonance frequency is experimentally verified by operating the same device at 2-30 Hz external vibrations[21].

In 2013,Anthony G. Fowlerl, S. O. Reza Moheimanil and Sam Behrens proposed another design in which they used ultrasonic excitation to generate power. But in that case they used electrostatic transducer. They were able to produce 120 mV in a device volume of 100 mm<sup>3</sup> at an ambient frequency of 110 Hz. The disadvantage is that a source of electric charge is required to bias the transducers before energy can be harvested by the system [22].

In 2013, Zhong Liang Li, Meng Di Han, and Hai Xia Zhang, from Institute of Microelectronics, Peking University, CHINA, proposed another design in which they used array of permanent magnets instead of a single block. The fabrication was easy but still there

is a scaling problem because of use of array of magnets. When the system vibrates because of improper synchronization the net magnetic flux is distorted [23].

#### **2.4 Classification of electromagnetic microgenerators and comparison of their performances**

A comparison of the various electromagnetic microgenerator designs discussed in Section 2.3.3 is presented in Table 2.1 - 2.2. The electromagnetic generators can be classified according to their moving element part, coil and magnet shapes, input vibration and /or the device volume.

The electromagnet generators can be discretely assembled generators with macro scale high-performance bulk magnets and multi-turn coils or micromachined generators with micromachined magnets, a planar coils and micromachined springs. Also there are some generators which are partially micromachined. The micromachined generators may have low output power and voltage compared to the assembled generators, due to the relatively poor properties of magnet, the limitations on the number of turns of the micro coil and the restricted .The objective of the current research is to develop an efficient design of an electromagnetic microgenerator that can harvest a low amplitude of vibration and frequency and able to generate power enough for remote sensing systems around  $100\mu\text{w}$  similar to the one proposed by Williams et. al.[25]. Having considered the designs that have been reported in the literature to date, the author has come to the conclusion that the objective can be met only through a design that incorporates the following key features.

- Design a compact suspension system with low mechanical damping by using material with low mechanical hysteresis loss, such as Si.
- Design different membrane configurations to get low natural frequency and low air damping with the aid of COMSOL modelling.
- Increasing the membrane deflection and the linear movement. The membrane should be designed so that the resonant frequency of the device matches the vibration frequency of the driving source using higher remanence permanent magnet like NdFeB and making the magnet size as large as possible within the device size.
- Increasing the number of turns on the coil and that could be achieved by using narrower tracks in the planar coil or using 3D folded coil.

Ref (year)	Moving element shape / material	Coil shape / Material	Magnet shape / Material	Resonance frequency ( Hz )	Power ( $\mu$ W )	Device Volume	Device features
<b>Amarithajah and Chandrakas</b>				2	400		Moving coil / discrete components
<b>El-hami et.al. (2001)</b>	Planar steel cantilever Beam	Wire coil	NdFeB	322	530	240 mm <sup>3</sup>	Moving magnet / Not a micromachined
<b>Ching et.al. (2002)</b>	Laser micromachined spiral copper	Wire copper coil		110	830	1 cm <sup>3</sup>	Moving magnet / same as Li et.al device/
<b>Kulah and Najafi</b>	Silicon Diaphragm	PCB	NdFeB	2511000	2.5	4 cm <sup>3</sup> , 2 cm <sup>3</sup>	Moving magnet
<b>Glynn-Jones et.al. (2004)</b>	Cantilever beam	Integrated coil	NdFeB	322	180	0.83 cm <sup>3</sup>	Moving magnet / partially micromachined
<b>Koukharenko et.al. (2006)</b>	Silicon cantilever paddle	Wound coil	NdFeB	1615	104 nW	100mm <sup>3</sup>	Moving coil/ micromachined device

**Table 2.1 Comparison of performance of various electromagnetic microgenerators**

Ref(year)	Moving element shape / material	Coil shape / Material	Magnet shape / Material	Resonance frequency ( Hz )	Power ( $\mu$ W )	Device Volume	Device features
<b>Pan et.al.(2006)</b>	Silicon membrane	Cu planner coil	Sputtered (FePt) magnet	60	100	0.45cm <sup>3</sup>	Moving magnet/ micromachined gen.
<b>Wang et.al.(2006)</b>	Copper spring	2 layer Cu coil	NdFeB	125			Moving Magnet
<b>Serre et. al. (2008)</b>	Polyimide film	Aluminum planner coil	NdFeB	360			Moving magnet
<b>Saha et. al. (2008)</b>	No chemical beam	Wound coil			200 nW	0.4cm <sup>3</sup>	Moving coil
<b>S. Turkilmaz(2011)</b>	Silicon membrane	Cu palner coil	NdFeB	200	3.21uW		Moving coil/moving magnet
<b>Anthony G. Fowlerl (2013)</b>	Silicon membrane	Copper coil		110		2cm <sup>3</sup>	Moving coil/moving magnet

**Table 2.2 Comparison of performance of various electromagnetic microgenerators**

## 2.5 Compact suspension system

Silicon micro beam mass structures are mechanical structures where linear elastic theory is generally applicable. However, to fabricate and use them as a functional system against a set design of specifications is extremely complicated due to their small sizes. A number of groups have reported the application of FEA for modelling the static and dynamic characteristics of microstructures [15, 25].

Tschan and Rooij [26] reported the characterization and modeling of three different designs of beam-mass structures for piezoresistive accelerometer. Four and two beam bridges and cantilever beams are shown in Fig.2.1 FEA were employed for the modelling of their vibration modes.

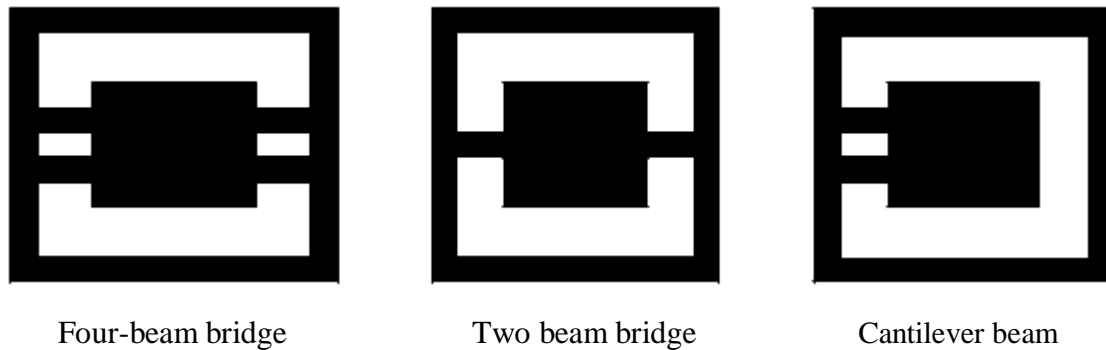


**Fig.2.1 Design of beam-mass structures.**

The FEA of these designs revealed that the beam thickness is the most critical parameter among the structure dimensions; for example, a small variation of  $0.5 \mu\text{m}$  was shown to change the sensitivity by 12% and the resonant frequency by 9%. The cantilever is the most sensitive structure, but its second and third modes are very easy to excite. For the four-beam bridge structure, the second mode is harder to excite when the distances between the two bridges are widened; consequently, the sensitivity along the y axis decreases. The opposite case occurs when the two bridges are brought together to form the two-beam bridge structure. Thus, the four-beam design is preferred over its two-beam counterpart due to its lower cross axis symmetry.

Puers and Lapadatu [27] carried out an investigation of the characteristics of various beam mass structures as a suspension system. As shown in Fig.2.2, four different structures were proposed in their comparative study using FEA. The dimensions of the mass and the thickness of the beams are same for each structure.

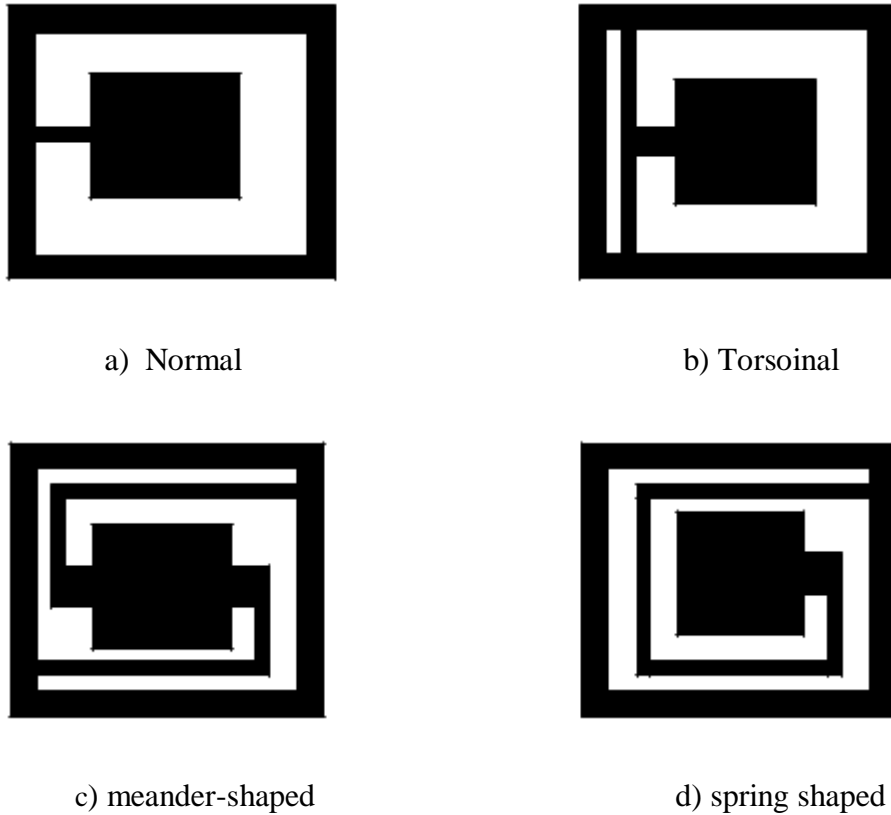


**Fig.2.2 Different suspension structures.**

Puers and Lapadatu [27] presented the characteristics of each structure as follows: a) the normal structure, which is a cantilever beam, has a cross sensitivity as much as half of its main sensitivity, i.e. the sensitivity in Z direction; b) the torsional beam has the smallest main sensitivity and very high cross sensitivity; however, if the width of the arm is reduced to the value of its thickness, the cross sensitivity decreases significantly; c) the meander-shaped structure has a main sensitivity close to the value of normal beam, while it exhibits extremely low cross sensitivity which can be further reduce by adding two more arms to the mass

structure; d) the spring shaped structure is the most sensitive one; however, its cross sensitivity is 50% of the main. For all the structures above, the sensitivities can be modified by adjusting the physical parameter such as length, width and thickness of the beams, but the essential vibrational characteristics remain unaffected.

## **2.6. Spring design objectives and considerations**

One of the most significant improvements of the electromagnetic microgenerator efficiency is to optimize the spring design. According to the literature there are some limitations that should be considered when a spring is design to be used in the electromagnetic microgenerator:

- The mechanical damping should be reduced by using a spring fabricated from a material with a low mechanical hysteresis loss, such as Si. This would be a significant improvement on the previous use of polyimide membrane spring.
- The deflection and the linear movement of the spring could be increased by employing a cantilever spring. Meandering spring design considered as the spring element in a meandering cantilever is longer than other designs allowing the spring to deflect further. The spring must have a maximum deflection within the generator size to make the magnet moves as close as possible to the coil to increase the induced flux.
- The spring should be designed so that the resonant frequency of the device matches the vibration frequency of the source.

Therefore, this research is investigating the spring designs for the use in power generating devices. Cantilever spring shape is considered to increase the linear movement. Different shapes of meandering and L-shaped springs with low resonance frequency are modelled and simulated with the aid of COMSOL finite element simulation software. Studying and investigating different materials to select the material with low mechanical losses.

## 2.7 Magnetic circuit

Magnetic circuit is the sum of the total number of paths the magnetic flux may follow as it passes from and returns to its point of origin. A magnetic circuit includes the magnetic flux source (basic permanent magnet) and any pole pieces or any ferromagnetic parts that are carrying some portion of the flux.

### 2.7.1 Permanent magnet

Due to the increasing availability of high energy permanent magnet materials, there has been much interest and studies in electromagnetic generators with permanent magnet excitation [16, 18, 20, 21]. Using the recently developed powerful permanent magnet material, Neodymium-Iron-Boron, further enhances the reliability and effectiveness of the generator. The permanent magnet establishes the flux in the coil. The coil should be located as close as possible to the magnet to minimize the amount of magnet flux leakage.

It is important to choose a type of magnet that will produce a strong flux density. Rare earth magnets are ideal for the electromagnetic microgenerator, and offer up to five times the magnetic energy density of conventional Alnico magnets which is an alloy of aluminium (Al), nickel (Ni) and cobalt (CO). Much of the recent progress made in the development of permanent magnet machines can be attributed to remarkable improvement of the properties of magnet materials. Following the successful development of samarium cobalt ( $\text{SmCo}_5$  and then  $\text{Sm}_2\text{Co}_{17}$ ) in 70s, there was some concern that the cost and availability of the principle constituents might limit the commercial success of these magnets. Attention was drawn to find new magnetic materials with superior properties to existing ferrite and alnico types. Earlier investigations involved using iron in place of cobalt with a variety of rare earth elements, but all the  $\text{R}_2\text{Fe}_{17}$  compounds have very low operating temperature [28]. A technical term, 'Curie temperature' ( $T_c$ ), is introduced to describe fundamental characteristic of magnetic materials. The term  $T_c$  expresses the temperature above, which spontaneous magnetization will not exist. The practical operating temperature for a magnet is well below  $T_c$  and yet  $T_c$  itself is only around  $125^\circ\text{C}$  for  $\text{Sm}_2\text{Fe}_{17}$  and around  $60^\circ\text{C}$  for  $\text{Nd}_2\text{Fe}_{17}$ .

Important progress was made in early 1980s.  $\text{R}_2\text{Fe}_{17}$  was modified to the ternary compound  $\text{R}_2\text{Fe}_{17}\text{B}$  which has tetragonal crystal symmetry and strong uniaxial magneto crystalline anisotropy. The Curie temperature for  $\text{R}_2\text{Fe}_{17}\text{B}$  is some  $200\text{-}300^\circ\text{C}$  higher than those of the

corresponding  $R_2Fe_{17}$  compounds. Then, development quickly focussed on  $Nd_2Fe_{17}B$ . This new alloy offers the highest saturation magnetization, and its  $T_c$  is over  $300\text{ }^\circ\text{C}$  [28]. The most compelling attribute of this compound, however, is that neodymium is considerably more abundant in the nature than samarium. It promises a significant saving in raw material cost by coupling neodymium with the use of iron as the transition metal.  $Nd_2Fe_{17}B$  is the basic compound for the modern family magnets known as neodymium-iron-boron, but various partial substations and modifications are commonly made to adjust the magnetic properties to suit practical applications.

It is known that the required magnet volume is inversely proportional to the energy product, i.e.  $B\text{-}H$  for a given air gap volume being magnetized to a certain flux density. Contours of constant energy product are rectangular hysteresis curve, usually drawn from property data sheet provided by magnet suppliers. The maximum energy product or  $(BH)_{\text{max}}$  of a given magnet occurs where the magnetization characteristic is tangent to  $BH$  hysteresis curve. As  $Nd\text{-}Fe\text{-}B$  has a large energy density than most of permanent materials, it has widely used in various types of electric machines.  $NdFeB$  magnets, also known as a rare earth iron magnets, are produced by a sintering process called rubber isostatic pressing (RIP). These high performance magnets are being used in both the electronics and power industries. Fig.2.6 shows a typical  $BH$  or hysteresis loop.

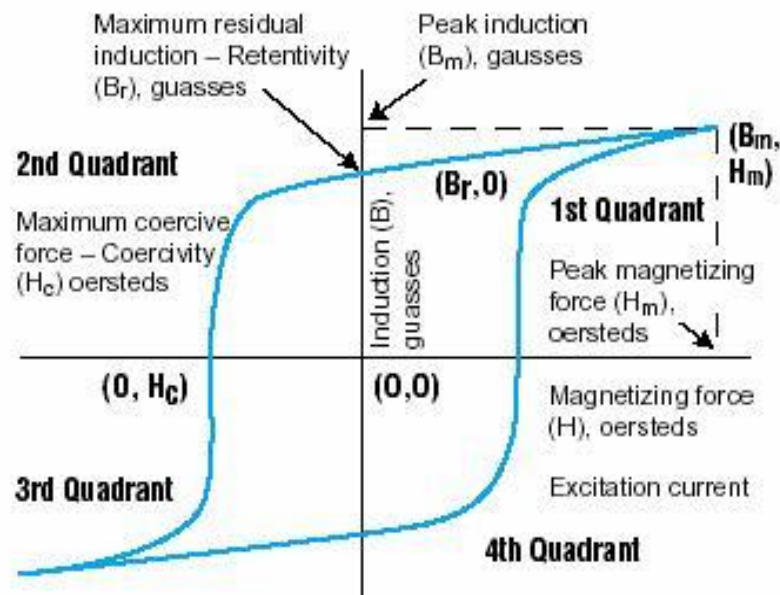
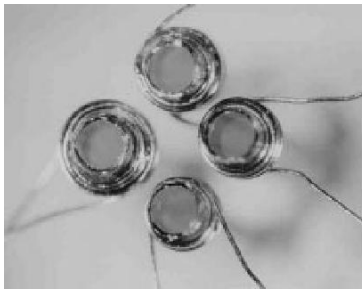


Fig.2.3 BH loop [29]

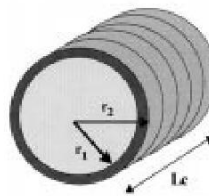
The flux density  $B$  is displayed on the vertical axis and the magnetizing force  $H$  is on the horizontal axis. Note that positive and negative values of both parameters are utilized. One variation of the BH loop is the demagnetization curve commonly used to display the properties of permanent magnetic materials. The “demag” curve only represents the second quadrant of the full BH loop. This is where the material has been magnetized.

## 2.8 Coil configuration design

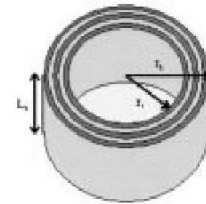
It has been established that a greater output can be achieved from the electromagnetic microgenerator by increasing the number of coil windings and reducing the impedance of the coil [25]. One of the improvements that have been suggested is to employ a wire wound coil. Coil parameters like coil configuration, diameter, wire material, number of winding turns and the shape of wire folding are studied.



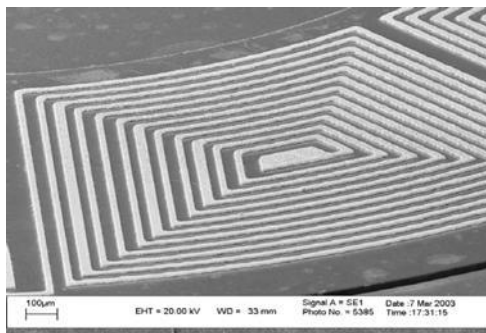
a)



b)



c)



d)

**Fig.2.4 Coil types in MEMS, a) Multilayer wire microcoils. b) Idealized solenoidal coil geometry. c) Idealized multilayer coil geometry. d) photograph showing top layer of a stator coil.**

There are two main types of coil in the literature. Firstly, the circular wire wound coil such as, solenoidal and spiral [Grant et.al.,2001; Kruusing,2002] as shown in Fig.2.9 a),b) and c), and secondly, the planar coil [Neagu et.al.,1997 ;Holmes et.al.,2005] that is fabricated by micromachining process as shown in Fig.2.9 d). The wound wire coils take advantage of reduced coil diameter. Coils with large inductance are difficult to implement in planar forms since many turns are required, resulting in large areas and large series of resistance. The planar coil is 2D coil while the folded coil is a 3D that makes the magnetic flux of the permanent magnet more accommodated by the folded coil.

## **2.9 Summary**

Vibration-to-electricity conversion offers the potential for MEMS and microelectronics devices to be self-powered in many environments. Low level vibrations occur in many environments including: large commercial buildings, automobiles, aircraft, ships, trains, and industrial environments. Electromagnetic microgenerators offer a well-established technique of electrical power generation over the piezoelectric and electrostatic generators.

A comparison of the various electromagnetic microgenerator designs has been discussed. The electromagnetic generators can be classified according to their moving element part, coil and magnet shapes, input vibration and or the device volume. The generators are also classified as macro size and micro size generators. A wide variety of spring/mass configurations with various types of material are used in the design of the electromagnetic microgenerator. High-performance bulk magnets and multi-turn, macro-scale coils are used in the macro size electromagnetic generators. Micromachined coils and micromachined magnet are used in the micromachined electromagnetic generators.

The general guide lines for efficient electromagnetic microgenerator design (as stated by Williams et.al.[25] has been formed. These guidelines will be described in chapter 3 for further study of the generator model through analytical investigations and parametric study.

A brief review about the springs design in the literature was presented. It was focused on improving the beam deflection of the spring from the first design with one cantilever beam to the design of a spring with a platform and four cantilever beams. It was found that a spring with four cantilever beams can achieve maximum large static deflection in the vertical direction and maximum stiffness to be along the axes other than in vertical direction.

A brief background of the permanent magnet and coil was given in this chapter to justify the selection of the NdFeB as a magnetic material and a 3D coil for the electromagnetic microgenerator.

## CHAPTER 3

### ANALYSIS OF AN ELECTROMAGNETIC MICROGENERATOR DESIGN

#### 3.1 Introduction

In this chapter an extensive analytical investigation develops an efficient design of an electromagnetic microgenerator. An analytical model is developed and then used for investigating the optimum design parameters to get maximum power output. A magnetic circuit concept is used in the analytical study. A description of the basic operating principles of the electromagnetic microgenerator is presented.

This chapter focuses on the development of the electromagnetic generator. The two designs depending upon the whether the coil or the magnet will be vibrating will be considered. Firstly in case of model consisting of a moving magnetic mass mounted on a suspension structure which allows a change of flux linkage with a coil deposited beneath the moving mass. For this case the EMF is given by the following equation:

$$\epsilon = -N \frac{d\phi}{dt} \dots \dots \dots (3.1)$$

Where,  $\epsilon$  is the electromotive force (EMF) in volt,  $\phi$  is the magnetic flux,  $N$  is the number of turns of coil.

In the second design of moving coil rather than moving magnet the conductor is wound in a coil to make an inductor. The relative motion between the coil and magnetic field causes a current to flow in the coil. In the simple case of a coil moving through a perpendicular magnetic field of constant strength, the maximum electromotive force (EMF) across the coil is given by equation 3.2.

$$\epsilon = NBlv \dots \dots \dots (3.2)$$

where:

$N$  is the number of turns in the coil,  $B$  is the strength of the magnetic field,  $l$  is the length of one coil ( $2\pi r$ ),  $v$  is the velocity of the coil through the magnetic field.

In practice a moving magnet design is simpler to fabricate as it avoids making electrical connection to the mass. There are two significant strengths to electromagnetic implementation. First, no separate voltage source is needed to get the process started. Second, the system can be easily designed without the necessity of mechanical contact between any

parts, which improve reliability and reduce mechanical damping. The moving magnet being attached with the spring will increase the seismic mass of the system and then increase the electrical power. This type of converter could be designed to have very little mechanical damping.

### 3.2 Analytical model proposed

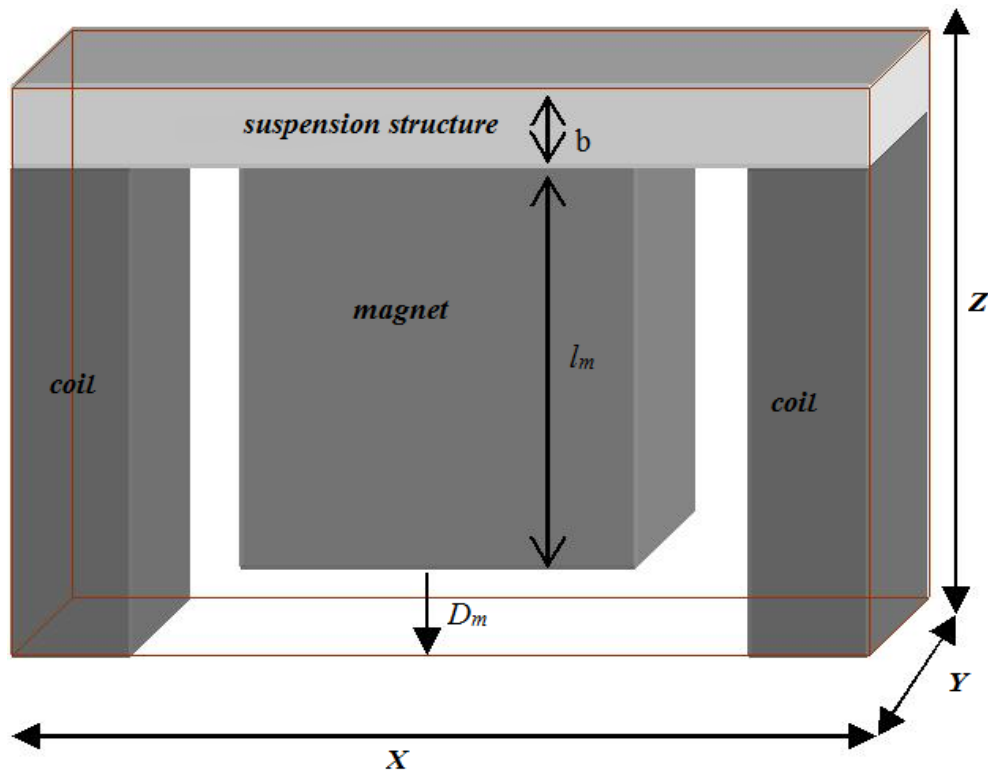


**Fig 3.1 Schematic of an electromagnetic generator**

A schematic of the electromagnetic generator is shown in Fig.3.2. The intention in this stage is not to go into details of MEMS fabrication steps for such a device, but to consider the operation principles and to understand the various design constraints. In this structure it is assumed that the coil remains fixed while the magnet moves in response to the vibration. Since the magnet has greater mass than the coil, movement of the magnet has more beneficial than movement of the coil. The available mechanical energy will depend on the level of vibrations and acceleration to which the device is subjected. However, the maximum displacement  $D_m$  is given by the difference between the external dimension of the generator,  $Z$ , the spring thickness  $b$  and the magnet length  $l_m$ . Assuming a sinusoidal vibration and

expressing the peak displacement of the mass as  $D_m = (Z-b-l_m)$ , the velocity,  $v$  of the mass can be expressed in terms of the input vibration and the mass displacement:

$$v = \omega D_m \dots\dots\dots(3.3)$$

$$v = \omega(Z - b - l_m) \dots\dots\dots(3.4)$$

The power delivered to the resistive load,  $R_L$ , can then be obtained from,

$$P = \frac{1}{2} i^2 R_L \dots\dots\dots(3.5)$$

Where  $i$  is the induced current through the circuit and  $R_L$  is the load resistance. The expression of the induced current,  $i$  is given by,

$$i = \frac{\epsilon}{R_L + R_C} \dots\dots\dots(3.6)$$

In this equation,  $R_C$  is the coil resistance and  $\epsilon$  is induced electromotive force (emf) on the coil defined by,

$$\epsilon = -N \frac{d\phi}{dt} \dots\dots\dots(3.7)$$

$$\text{As } \phi = BA, \quad dA = lds, \quad d\phi = BdA = Bl ds$$

$$\text{Now, } \epsilon = N \frac{d\phi}{dt} = NBl \frac{ds}{dt} = vNBl = \omega D_m NBl \dots\dots\dots(3.8)$$

$$P = \frac{R_L}{2} \left( \frac{\epsilon}{R_L + R_C} \right)^2 \dots\dots\dots(3.9)$$

$$P = \frac{R_L}{2} \left( \frac{vBl}{R_L + R_C} \right)^2 \dots\dots\dots(3.10)$$

Design analyses of the electromagnetic microgenerator have revealed a number of points:

1. The output power is proportional to the proof mass. This is not immediately obvious from the expression for power in equation 3.9. However, increasing the magnet mass will increase the magnetic field density ( $B$ ) and this would significantly increase the predicted power output.
2. The power output is proportional to the square of the frequency of the driving vibrations. This follows directly from equation 3.9 because the input frequency is included in calculating the generator velocity ( $v$ ) as it can be seen from equation 3.4.
3. The power output is proportional to the square of the coil length. This follows from equation 3.9.

4. The power output is inversely related to the square of the coil resistance. Again, this follows from equation 3.9.

Potential advantages of this design are:

1. The spring is selected to be a cantilever type to increase the mass deflection and the linear movement of the spring and then reduce the mechanical damping.
2. The magnet is decided to be a moving magnet and attached to the middle of the spring to increase the inertial mass of the generator.
3. The coil is decided to be a wound coil to get large number of turns to accommodate the magnetic field.

### 3.3 General Principle of operation

The operating principle of the device is as follows: when the housing is vibrated, a mechanical input force feeds into a mechanical system, the mass moves relative to the housing and energy is stored in the mass-suspension system. This relative displacement, which is sinusoidal in amplitude, causes the magnetic flux to cut the coil. This in turn induces a voltage on the coil due to the varying flux linkage within the motion between the magnet and the coil as stated by Faraday's law of induction. The electrical system involved is simply a first-order LR circuit with the inductance of the coil ( $L$ ) in series with the load resistance and parasitic resistance of the coil ( $R$ ). In the former case, the amount of electricity generated depends upon the strength of the magnetic field, the velocity of the relative motion and the number of turns of the coil.

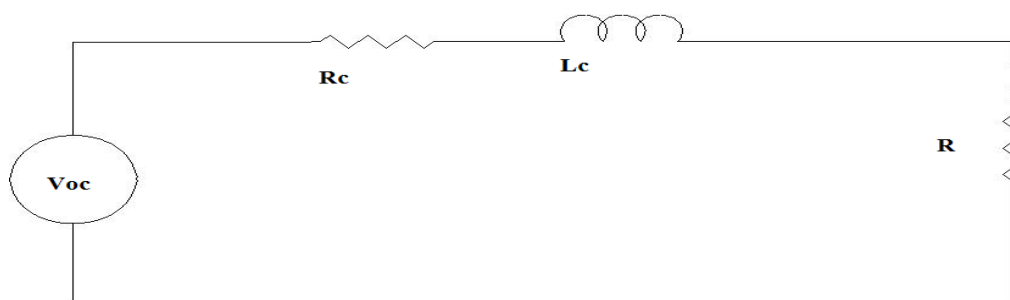


**Fig. 3.2 Simplified equivalent circuit model of electromagnetic microgenerator**

If a simple resistive load is attached to the electromagnetic microgenerator as shown in Fig. 3.2, an AC voltage ( $V_{load}$ ) will appear across the load. The average power delivered to the load is then should be rectified and conditioned by power electronics. However, the circuit shown in

Fig 3.2 gives an easy and useful calculation of power generation simply  $P = V_{load}^2 / 2R_{load}$ . In reality, a simple resistor is not a very useful load. The voltage should be rectified and conditioned by power electronics. However, the circuit shown in Fig 3.2 gives an easy and useful calculation of power generation.

### **3.4 Summary**

In this chapter a proposed design was shown. The model was extensively analysed to obtain certain set of equations given above. Depending upon the equations certain points are noted out which characterizes the output power of the model. The practical advantages of the model over the other models described in the literature are discussed. An electromagnetic microgenerator whose operating principle is based on the relative movements of a permanent magnet with respect to a coil has been proposed.

## Chapter 4

### Modelling and Simulation

#### 4.1 Introduction

This chapter presents the different designs of the suspended bridges. The basic theory of the static and dynamic modelling of the micromechanical structures were studied and presented. The design objectives and specifications of the suspension designs to be used in the electromagnetic micro generator were discussed. The key design parameters such as static deflection, spring constant, resonant frequency, and dynamic range were investigated. Cantilever spring shape is considered to increase the linear movement. Different shapes of meandering and L-shaped springs with low frequency resonating springs are modelled and simulated with the aid of COMSOL finite element simulation software. Studying and investigating different materials to select the material with low mechanical losses is presented. Then the different simulated results of the voltage generated are shown by considering different parameters.

#### 4.2 Theoretical considerations of the suspension design

##### 4.2.1 Static considerations

The cantilever beam in the flat spring is assumed to be straight and have a rectangular cross section. As shown in Fig.4.1, the beam is assumed to be long in proportion to its thickness and is not excessively wide. All loads and reactions are to be perpendicular to the axis of the beam and lie in the longitudinal plane of symmetry of the beam.

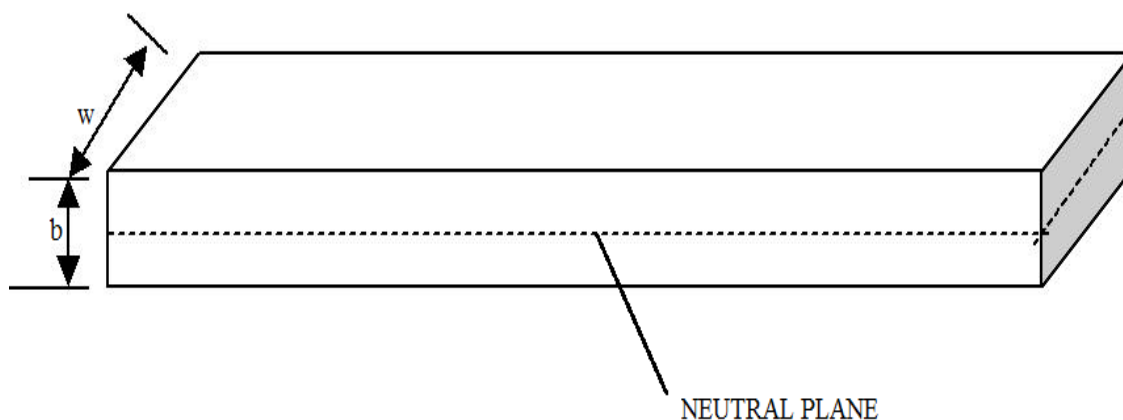


**Fig.4.1 Cantilever beam in the original position**

### 4.2.1.1 Stress and strain

The stress on a cantilever beam is  $Stress (T) = F / A$  where,  $F$  = Applied force and,  $A$  = cross-sectional area of the beam and the strain result of an applied force and it is expressed as  $Strain(\epsilon) = \Delta l / l$  where,  $\Delta l$  = extension and,  $l$  = original length of the beam. So the relationship of the strain and the stress of a cantilever beam can be expressed as  $E = T / \epsilon$ , where  $E$  is the elasticity or the young's modules of the beam material. As shown in Fig.4.1, for a beam with rectangular cross section and with a width of  $w$  and a thickness of  $b$  the moment of inertia is  $I = wb^3 / 12$ .

### 4.2.1.2 Deflection of the flat spring

The static deflection  $D$  is given by the basic expression of an undamped spring-mass system:

$$D = F / k \dots\dots\dots (4.1)$$

where,  $F$  is the applied force and  $k$  is the spring constant.

The deflection of the cantilever beam for the case of a concentrated force  $F$  applied at the free end of the beam as shown in Fig.4.2 is given by Equation (4.2):

$$D = \frac{Fl^3}{3EI} \dots\dots\dots (4.2)$$

Where  $l$  is the length of the beam,  $I$  is the second moment of area of the cross section of the beam, and  $E$  is Young Modulus of the material of the beam.

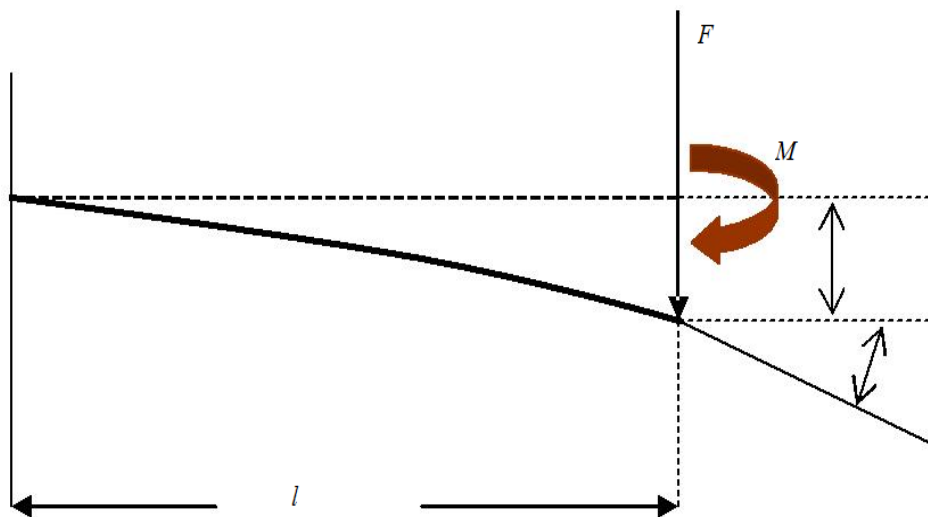


**Fig. 4.2 Basic diagram of the deflection of cantilever beam with concentrated force  $F$  applied at the free end of the beam and Moment  $M$  applied at the free end of the beam**

The spring constant can be given by equation 4.3[30]:

$$K = 4Eb^3w/l^3 \dots\dots\dots(4.3)$$

Where  $b$ ,  $w$  and  $l$  are the thickness, width and mean length of the spring beam and  $E$  is the modulus of elasticity of the spring material. By substituting equation (4.3) in equation (4.1) gives the static deflection for the suspended mass

$$D = Fl^3 / 4Eb^3w \dots\dots\dots(4.4)$$

## 4.2. 2 Dynamic considerations

### 4.2. 2.1 Vibration of a spring mass system

Fig. 4.3 shows a typical spring mass system which consists of a mass  $m$  restrained by a spring of stiffness  $k$  and a damper having viscous damping coefficient  $c$ . the mass is assumed to be constrained to move in the  $x$  direction, and the mass of the spring is assumed negligible compared with  $m$ . If the mass is excited by the external force  $F(t)$ , Newton's second law of motion can be applied to the system.

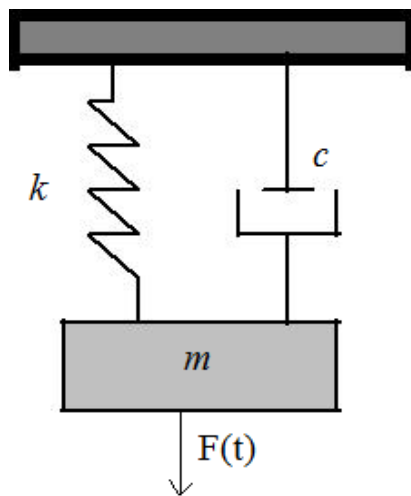


**Fig.4.3 Spring mass system with single degree of freedom**

The flat spring-mass structure is equivalent to an undamped spring-mass system if it operates in vacuum, or the damping caused by air is neglected. Without the external force  $F(t)$ , free vibrations will occur in the system when the mass is subject to an initial displacement or velocity. The natural frequency or resonant frequency of the suspension system is:

$$f = \frac{1}{2\pi} \sqrt{\frac{k}{m}} \dots\dots\dots(4.5)$$

### 4.2.3 Material selection

Large mass deflection and high resonance frequency of the flat spring are the goals of designing the spring and it is highly dependent on the material properties. In comparing different materials a few fundamental material properties are important like Young's modulus (E) which decides the stiffness of the spring. To achieve this, different materials have been considered. Their relevant properties are summarized in table 4.1 [31,32]. SU-8, Gallium Arsenide (GaAs) and copper (Cu) have lower young's modulus than silicon that make the spring able to give larger deflection with the same applied force. However, these materials have very low yield strength in comparison to the silicon yield strength. GaAs is an expensive material and requires a very difficult fabrication processes and SU-8 has the problem of removal after fabrication. Therefore, silicon was chosen as the preferred material for the spring as it has good mechanical properties such as high yield strength and low mechanical losses. At room temperature and under applied load, silicon can only be elastically deformed. Moreover silicon is relatively inexpensive material and has available standard processes of fabrication.

**Table 4.1 Properties of materials considered for the mechanical springs**

Material	Young's modulus (GPa)	Poisson's Ratio	Density (g/cm <sup>3</sup> )	Yield Strength (MPa)
Silicon	190	0.22	2.30	7000
Gallium Arsenide	75	0.31	5.3	2000
Copper	110	0.35	8.94	69
SU-8	3	0.22	1.19	179.4

### 4.3 Finite-Element Modelling

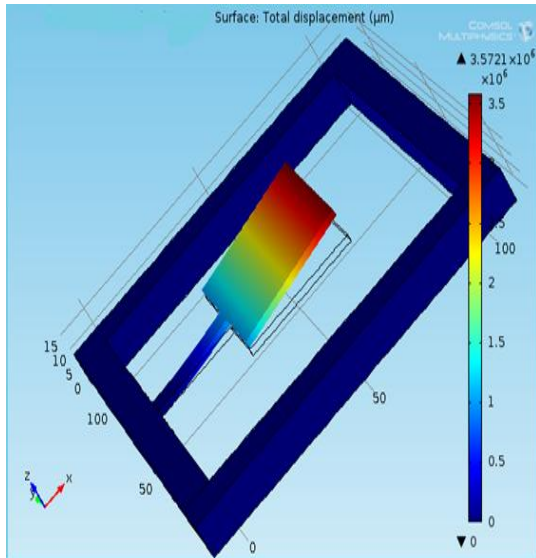
Much work has been dedicated to analytical and numerical modelling techniques for mechanical structures. Finite-element modelling is a very powerful tool for understanding the behaviour of the mechanical springs. The modelling was accomplished by utilising a commercial available finite-element software package, COMSOL 4.4. The first step in a finite-element procedure is to divide the domain of interest into number of smaller subdomain that contain of elements and nodes. The nodes are points at the intersection of the element boundaries. The finite element method uses an integral formulation at each point to create a

system of algebraic equations. An approximate continuous function is assumed to represent the solution for each element. The complete solution is then generated by connecting or assembling the individual solutions [33]. In general finite-element program for modelling should contain these steps:

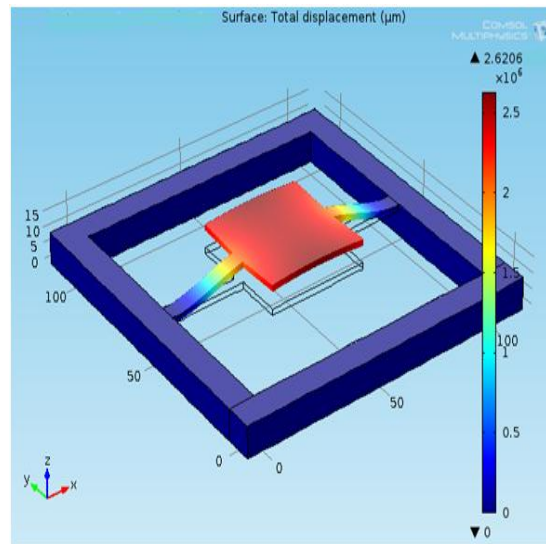
- The meshing of the problem (subdivide the geometry of the model into regions that can be represented by nodes and elements).
- The selection of the appropriate shape functions to represent the physical behavior of the elements. In COMSOL, this is done by selecting the element type which is responsible for the approximate continuous function representing the solution for each element.
- The assembly of the elements (constructing the global stiffness matrix to represent the entire problem).
- The application of the boundary and initial conditions (i.e. mechanical or electrical loading).
- To solve the set of algebraic equations simultaneously to obtain nodal results.
- The extraction of the important information such as displacement and electric potential.

### 4.3.1 Suspension model simulations

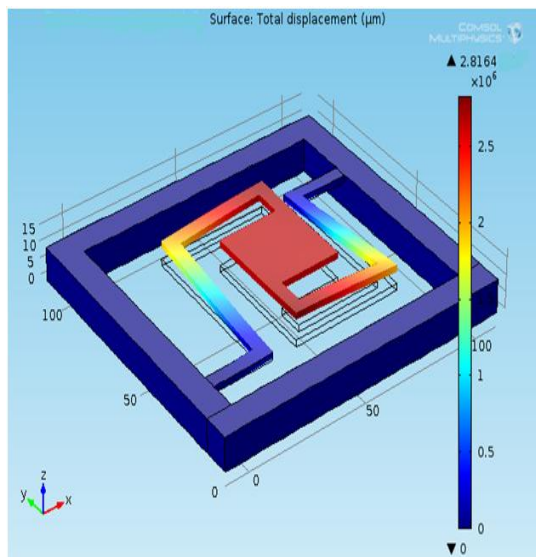
The different suspension designs are analysed and then simulated. The below figures show the simulation of the various designs.



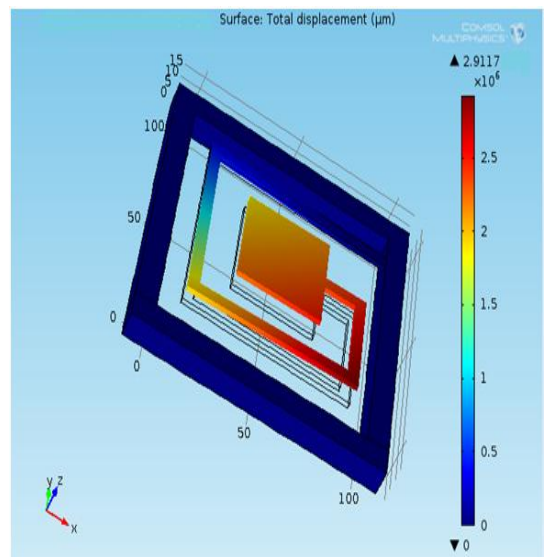
a)



b)



c)



d)

**Fig.4.4 COMSOL finite element models for the Suspension designs, a)1 beam(cantilever), b)2 beam , c)spring beam and d)multiple beam**

COMSOL structural static analyses were performed on the four spring shapes. The maximum static deflection under gravitational force was determined. In the first set of the structural analysis, the four springs have the same outer dimensions and same platform size but

different beam length and configuration. It is assumed that the type of material is fixed to silicon and applied to all spring's shapes. The mesh was created so that the highest density of nodes was on the beams and in the centre of the structure. The units used in the ANSYS software are in the “μmks” system where μm is used everywhere in place of m (meter) meaning that N (Newton) becomes μN (Kg. μ m/s<sup>2</sup>) and P (Pascal Pressure) becomes MPa (Kg / μ m.s<sup>2</sup>).

The simulated results are listed below in the form of table 4.2

**Table 4.2 Results of maximum deflection in z- direction**

Spring shape	1-beam bridge	2-beam bridge	Spring beam	Multiple beam
Deflection(μm)	3.57	2.62	2.91	2.81

The deflection of any structure depends upon the design of the structure. From our point of view we are designing the structures to have the maximum deflection.

The single beam bridge has the highest deflection of 3.5721 μm but the problem with single beam bridge is that it has the non linear deflection in z-direction that has been seen during simulation and also shown in fig 4.2 (a).

The two beam bridge has got less deflection than single beam bridge and is equal to the 2.6206 μm but the deflection is entirely in z direction that can be seen in fig 4.2(b).

The spring beam bridge has got more deflection than two beam bridge of the order of 2.9117 μm but the problem is it does not has the linear deflection in z-direction.

The multiple beam bridge has got the deflection nearly equal to the spring beam bridge but having more linerised deflection in z-direction.

In the entire simulations shown above the beam width is made constant to 10 μm but the effect of beam width also has to be analysed therefore various simulations has been done by varying the beam width and beam length the results of which are summarized below in the form of table 4.3. the table 4.3 a) shows deflection values for different beam lengths keeping beam width constant to 10 μm and table 4.3 b) shows deflection values for different beam widths.

**Table 4.3 a) deflections for different beam lengths**a) One beam bridge and two beam bridge (beam width=10  $\mu\text{m}$ )

Beam length ( $\mu\text{m}$ )	Deflection ( $\mu\text{m}$ )	
	One beam bridge	Two beam bridge
150	16.37	11.32
200	17.01	12.02
250	17.98	12.93
300	18.86	13.67

b) Spring beam bridge (beam width=10  $\mu\text{m}$ )

Beam length ( $\mu\text{m}$ )	Deflection ( $\mu\text{m}$ )
450	14.98
500	15.27
550	15.89
60	16.32

c) Multiple beam bridge (beam width=10  $\mu\text{m}$ )

Beam length ( $\mu\text{m}$ )	Deflection ( $\mu\text{m}$ )
300	14.563
350	14.982
400	15.20
450	15.86

**Table 4.3 b) deflections for different beam widths**

Beam width ( $\mu\text{m}$ )	Deflection ( $\mu\text{m}$ )			
	One beam bridge (beam length=150 $\mu\text{m}$ )	Two beam bridge (beam length=150 $\mu\text{m}$ )	Spring beam bridge (beam length=450 $\mu\text{m}$ )	Multiple beam bridge (beam length=300 $\mu\text{m}$ )
10	16.37	11.32	14.98	14.563
20	12.46	9.76	12.79	12.73
30	10.65	7.82	11.03	10.23
40	8.92	6.01	8.34	8.02

#### 4.4 FEA to calculate the magnet-coil separation

The objective of this analysis is the determination of the optimum position of the electric coil relative to the permanent magnet in the magnetic circuit. The optimum position of the electric coil is meant the position at which the magnetic induction field is at its maximum value. The only limitation of the distance of the coil and the magnet is the spring dimensions as the magnet is attached to it. In COMSOL simulation the applied distance is ( $x$ ) starts from  $200\mu\text{m}$  to  $500\mu\text{m}$ . The magnet is at the initial position.

The simulated results of magnetic field density are shown. The magnetic field is at maximum values in the middle of the magnet and as the separation distance is reduced the coil pole seems to be much closer to the highest density of the magnetic field. The simulated result of magnetic field density is shown in figure 4.5 by keeping the distance between the coil and the magnet is  $200\mu\text{m}$  and the rest of the results are shown in the figure 4.6.

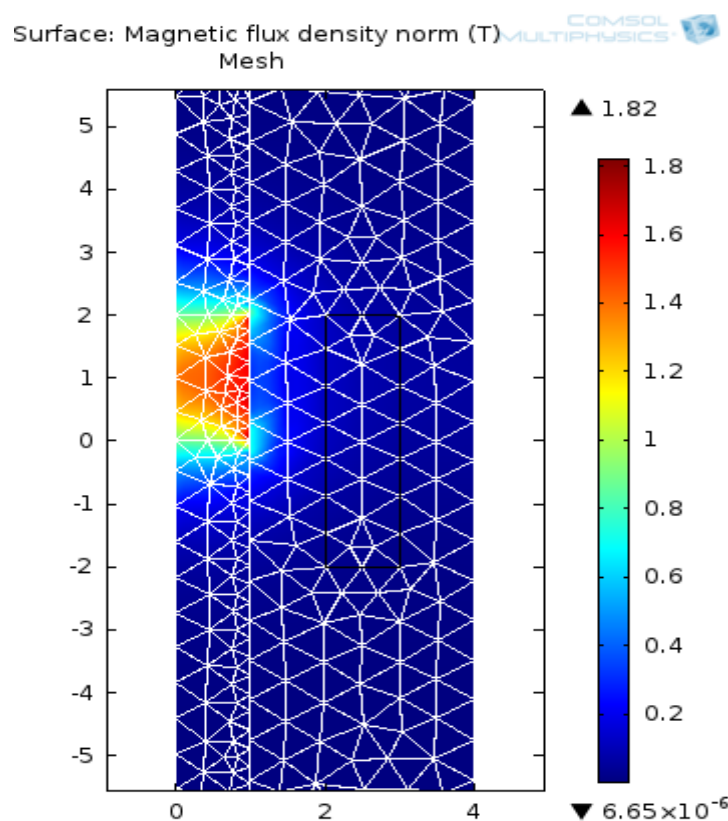


**Fig. 4.5** The magnetic induction field  $B$  at a distance  $200\mu\text{m}$ .

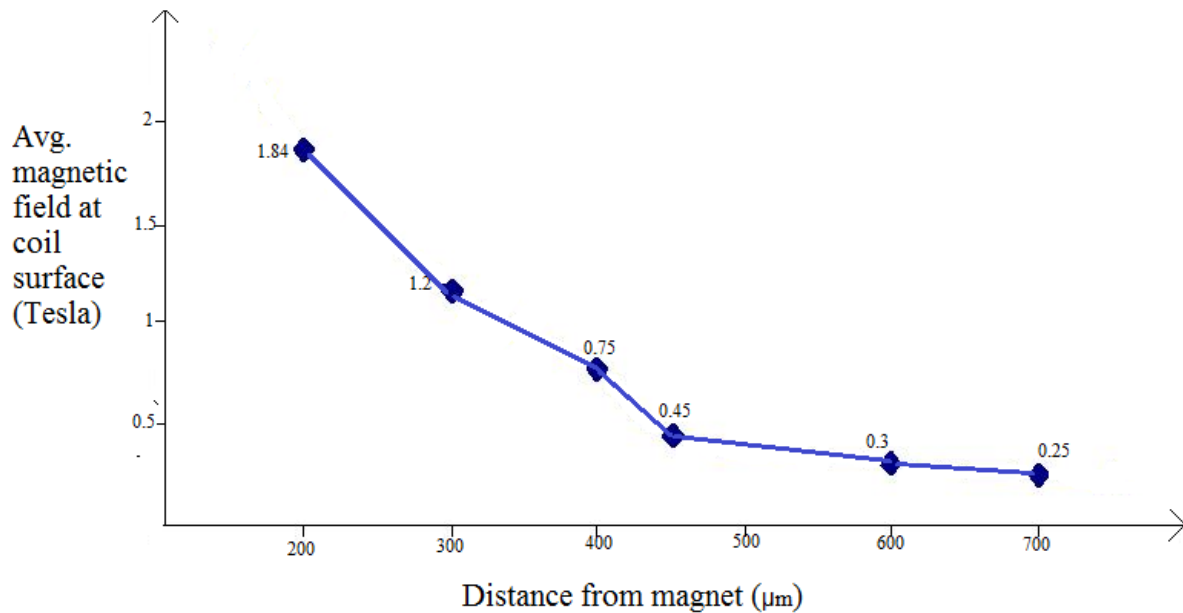
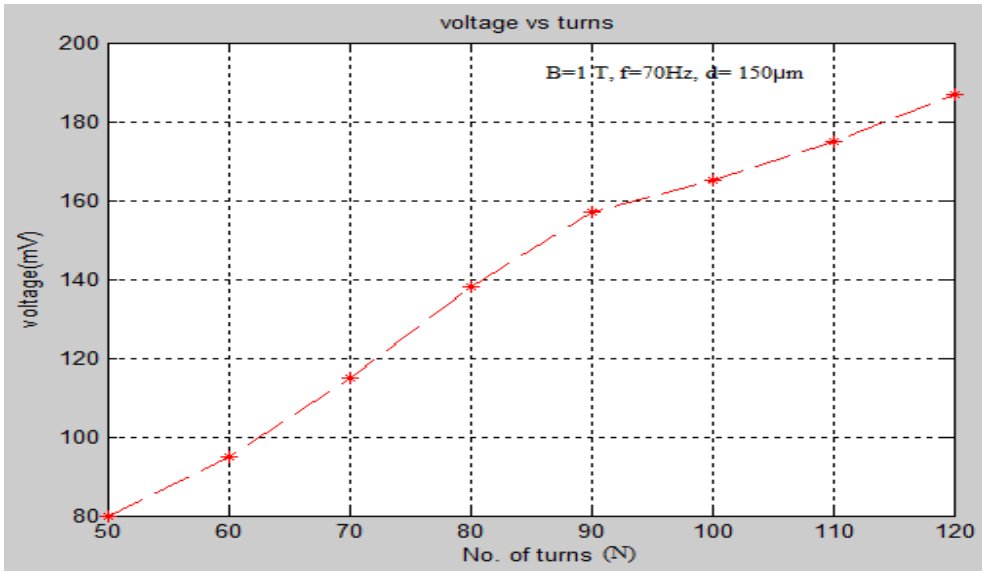


**Fig.4.6 COMSOL results of average  $B$  versus distance between the coil and the magnet**

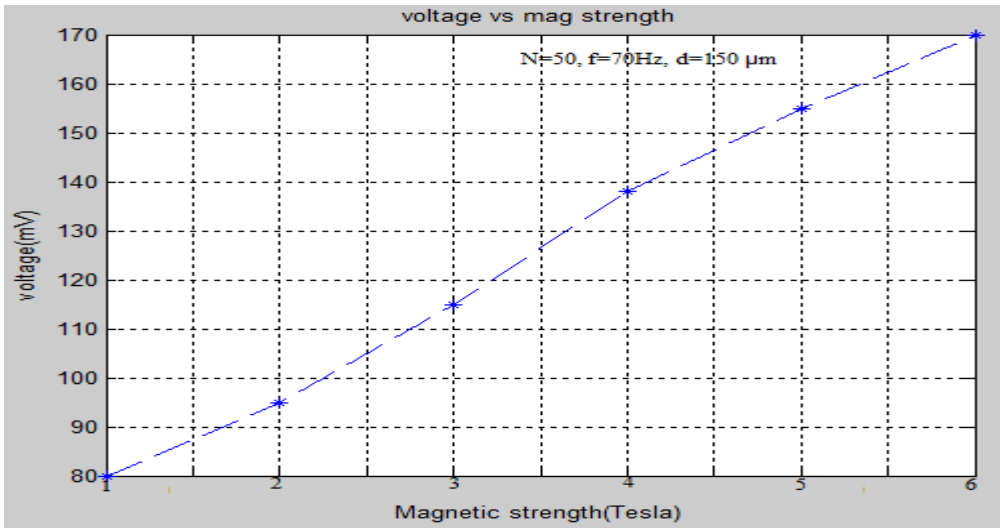
As shown in Fig.4.6 the magnetic field,  $B$  on the coil nodes seems to increase with the reduction in the distance between the magnet and the coil. The magnetic field density  $B$  in the coil pole is calculated by computing the magnetic field density along a number of nodes and taking the average. This indicates that the closer the coil to the magnet, the larger the induced magnetic field on the coil. However, the distance is limited by the spring dimension and the size of the generator. This shows that the magnetic field can be optimized by reducing the distance between the coil and the magnet.

#### 4.5 Simulated voltage

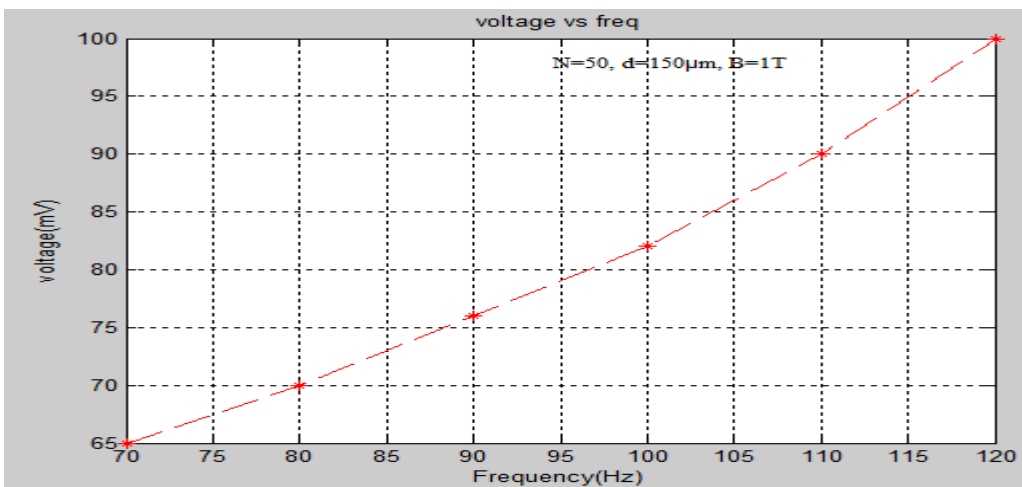
The voltage and output power generated by the electromagnetic power generator are obtained using the simulation results of the magnetic field from the section 4.4 and from the certain set of equations (3.3-3.9). The value of frequency is taken to be ambient (100Hz). An input velocity is given by equation (3.3). It is also assumed that the generator has a coil with  $N$  turns all of the same area  $A$  (and the magnet is moving in a variable velocity towards the coil. The applied displacements are taken from the structural analyses in chapter 4, table 4.3. Copper material is used for the coil. The output voltage is calculated using equations (3.8) and compared with the values of the simulation results. The figure 4.7 shows the simulation results of induced voltage for different parameters.



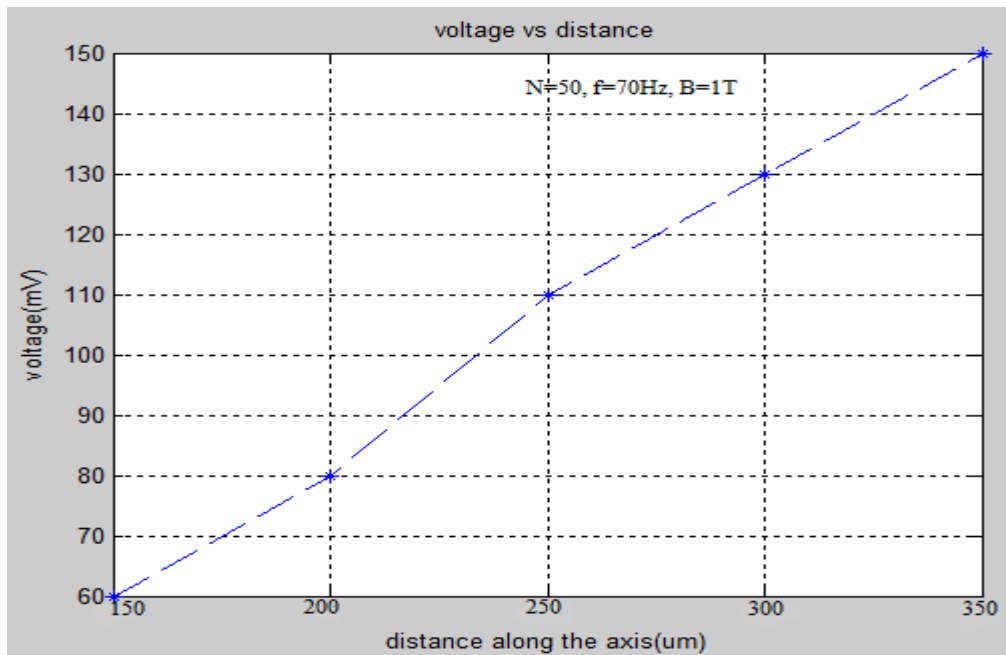
a)



b)



c)



d)

**Fig. 4.7 output voltage v/s a) no. of turns b)magnetic field c) frequency d) distance along axis.**

In Fig. 4.7 a), the output voltage increases with number of coil turns. From equation 3.8 and Fig.5.14a it is clear that an increase in the number of turns lead to an increase in the generated voltage. Fig. 4.7 b) clearly shows that the voltage increased as the magnet field strength is increased which results in more magnetic flux linkage with the coil. The effect of increase in frequency shows that the voltage is increased as the magnet velocity gave an increase in the magnetic flux rate ( $d\phi/dt$ ). The figure 4.7 d) shows higher the deflection of the magnet/membrane in the z-direction, greater will be the induced voltage.

#### 4.6 Summary

FEA was used to investigate the optimum location of the coil in relation to the permanent magnet. The results showed that the maximum magnetic field of 1.84 Tesla could be obtained on the coil if the coil is as close as 200 $\mu$ m to the magnet. By providing the FEA results and using voltage equation, the effect of varying the coil turns in the output voltage and power has been investigated.

## **CHAPTER 5**

### **CONCLUSION**

A comparison of the various electromagnetic microgenerator designs has been discussed through the literature review of this thesis and power supplies for MEMS devices have been briefly demonstrated. This thesis describes the design of a new electromagnetic microgenerator. The analysis of a suspension designs and the selection of a number of coils of the generator are also presented. The electromagnetic generators in the literature can be classified according to: their moving element part, coil and magnet shapes, input vibration and or the device volume. The general guide lines for efficient electromagnetic microgenerator design have been concluded. These guide lines was undertaken for further study the generator model through analytical investigations and parametric study. A brief review about the springs design was also presented. It was focusing on the improving of the beam deflection of the membrane from first design with one cantilever beam to the design of a platform with multiple beams. The improvements in deflection may be attributed to the reduced stiffness and increased beam length.

Using COMSOL magnetic analyses was conducted to characterize the permanent magnet at initial position. It is found that the magnetic field of the permanent magnet in the vertical direction is higher in magnitude than the magnetic field in the horizontal direction. FEA was then used to investigate the magnetic forces acting on the coil. The results showed that the maximum magnetic field could be obtained if the coil is as close as 100 $\mu$ m to the magnet.

#### **5.1 Comparison study of the electromagnetic microgenerator**

A comparison study between the electromagnetic generator in the literature and the electromagnetic generator in this thesis concluded that the generator presented in this thesis aims to generate significant power from low frequency.

Table 5.1 shows a comparison between the reported electromagnetic generators based on moving magnet. The comparison based on the resonance frequency, output power, output voltage and the volume of the generators.

**Table 5.1 Comparison between the reported electromagnetic generators based on moving magnet.**

Ref.(Year)	Resonance frequency ( Hz )	Power ( $\mu$ w )	Voltage	Device volume	
Shearwood et.al, (1997)	440	0.3		$5 \times 5 \times 1 \text{ mm}^3$	Measured
Ching et.al. (2002)	110	830		$1 \text{ cm}^3$	Measured
Kulah and Najafi (2004)	25, 11000	2.5, 4nw		$4 \text{ cm}^3, 2 \text{ cm}^3$	Simulated/Measured
Glynn-Jones et.al.(2004)	322	180		$0.84 \text{ cm}^3$	Measured
Pan et.al.(2006)	60	100		$0.45 \text{ cm}^3$	Measured
Wang et. al.( 2007)	121.25		60mV		Measured
Serre et. .al (2008)	360	200nw			Measured
Kulkarni et.al. (2008)	60	584nw		$150 \text{ mm}^3$	Measured
The electromagnetic generator of this thesis	90		160 mV	$1 \times 1 \times 2 \text{ mm}^3$	Simulated

## 5.2 Suggestions for Future Work

Electromagnetic microgenerator represents an ideal power solution for MEMS applications because of its potential to power MEMS devices indefinitely. However, more work need to be done in the field of vibration to electricity conversion. A few issues that can be an extension of this research are presented below.

Only limited numbers of design configurations have been evaluated in this study. Other design configurations that have better mechanical characteristics, and potentially higher power outputs should be evaluated. More effort needs to be done to improve the electromagnetic microgenerator design for example the suspension design could be designed with holes on the beams to allow vacuum operation or consider using different materials.

A more detailed simulation study of the deflection would help to improve its stiffness further in achieving high deflection. More comprehensive work is required in modelling and fabrication of the membranes and studying their effects on the output power. Work is needed to consider the spring behaviour under other environmental vibrations.

Detailed electromagnetic simulation studies of the coil and the magnet are needed such as:

1. changing the magnet size and calculate the  $B_x$  and  $B_y$  and also  $B$  at the coil node
2. changing the coil size and calculate the  $B$  at the coil nodes.
3. Adding a core made of ferromagnetic material to the coil and do more simulation work to calculate the  $B$ .
4. From the coil theoretical model we can vary the coil parameters and get different length and thickness of the coil to apply it to the COMSOL analysis.

The most challenging aspect of any MEMS project is the design of the processing steps that are required to fabricate the device. Many problems that are not foreseen during the design phase are very likely to crop up when attempting to fabricate the device. Only by fabrication and evaluation of a number of prototype electromagnetic microgenerators, the proof of concept of the electromagnetic microgenerator could be established. Experimental results can be used to validate the FEA results.

## References:

- [1] H. Kulah and K. Najafi, "An Electromagnetic Micro Power Generator for Low-Frequency Environmental Vibrations," 17<sup>th</sup> IEEE International Conference on Micro electro mechanical Systems (MEMS '04), Maastricht, The Netherlands, pp. 237-240, January 2004.
- [2] A. Muhtaroglu, A. Yokochi, A. von Jouanne, "Integration of Thermo electrics and Photo voltaics as Auxiliary Power Sources in Mobile Computing Applications", Journal of Power Sources, Vol.177,No.1,pp.239-246,February2008.
- [3] Roundy S., Wright P.K., and Rabaey J., A study of low level vibrations as a power source for wireless sensor nodes. Computer Communications, 2003, pp. 1131-1144.
- [4] Lee S. H., Development of high-efficiency silicon solar cells for commercialization. Journal of the Korean Physical Society, Aug. 2001. 39(2): p.369- 373.
- [5] Starner T., Human-powered wearable computing. IBM Systems Journal, 1996, pp. 618-629.
- [6] Glynne-jones P., Beeby S.P., and White N.M., Towards a piezoelectric vibration-powered microgenerator. IEE proceedings, 2001.
- [7] Ottman G. K., Hofmann H. F., Bhatt A. C., Lesieutre G. A. 2002. Adaptive piezoelectric energy harvesting circuit for wireless remote power supply. IEEE Transactions on Power Electronics, vol.17, no.5, 2002, pp.669-76.
- [8] Meninger S., Mur-Miranda j.O., Amirtharajah R., Chandrakasan A. P., and Lang J.H.,Vibration-to-Electric Energy Conversion. IEEE Trans.VLSI Syst, 2001, pp. 64-76
- [9] Amirtharajah R.,Meninger S.,Mur-Miranda J.O.,Chandrakasan A.,Lang J., Micro power programmable DSP powered using a MEMS-based Vibration-to-Electricity Energy converter. In IEEE International Solid State Circuits Conference. 2000, pp.362-363.
- [10] El-hami M., Glynne-Jones P., White N.M., Hill M., Beeby S.P., James E., Brown A.D. , and Ross J.N., Design and fabrication of a new vibration-based electromechanical power generator. Sensors and Actuators A, 2001, pp. 335-342.
- [11] Ching N. N. H., Wong H.Y., Li W. J., Leong P.H.W., and Wen Z., A laser-micromachined multi-

modal resonating power transducer for wireless sensing systems. *Sensors and Actuators*, 2002, pp. 1-6.

[12] Glynne-Jones P., Tudor M.J. , Beeby S.P., White N.M., An electromagnetic, vibration-powered generator for intelligent sensor systems, *Sensors and Actuators A* , 2004, pp. 344–349.

[13] Beeby S. P., Tudor M. J., Koukharenko E., White N. M., O'Donnell T., Saha C., Kulkarni S. and Roy S., Micromachined silicon generator for harvesting power from vibration. in *Proc. Transducers 2005*. (Seoul, Korea).

[14] Pan C.T., Hwang Y.M., Hu H.L., Liu H.C., Fabrication and analysis of a magnetic self-power microgenerator, *Journal of Magnetism and Magnetic Materials*, 2006, pp. 394–396.

[15] Wang P.H, Dai X.H., Fang D.M., and Zhao X.L., Design, fabrication and performance of new vibration-based electromagnetic micro power generator. *Microelectronics Journal*, 2007. pp. 1175-1180.

[16] Serre C., Pe´rez-Rodrı´guez A., Fondevilla N., Martincic E., Martı´nez S., Morante J., Montserrat J., Esteve J., Design and implementation of mechanical resonators for optimized inertial electromagnetic microgenerators, *Microsyst Technol* , 2008, pp. 653–658.

[17] Saha C.R., O'Donnell T., Wang N., McCloskey P., Electromagnetic generator for harvesting energy from human motion, *Sensors and Actuators A* ,2008, pp. 248–253.

[18] Sari I., Balkan T., Kulah H., An electromagnetic micro power generator for wideband environmental vibrations, *Sensors and Actuators A* ,2008, pp. 405–413.

[19] Kulkarni S., Koukharenko E., Torah R., Tudor J., Beeby S., O'Donnell T., Roy S., Design, fabrication and test of integrated micro-scale vibration-based electromagnetic generator, *Sensors and Actuators A* , 2008, pp. 336– 342.

[20] Turkyilmaz, S. ; Kulah, H. ; Muhtaroglu, A. “Design and Prototyping of Second Generation METU MEMS Electromagnetic Micro-Power Generators” ©2010 IEEE

[21] S. Turkilmaz and O.Zorlu, “ An Electromagnetic Micro-Power Generator for Low Frequency Vibrations with Tunable Resonance” © 2011 Elsevier Ltd.

- [22] Anthony G. Fowler<sup>1</sup>, S. O. Reza Moheimanil<sup>2</sup>, and Sam Behrens<sup>2</sup> "A MEMS ELECTROMAGNETIC ENERGY HARVESTER USING ULTRASONIC EXCITATION" 2013 IEEE/ASME International Conference on Advanced Intelligent Mechatronics (AIM) Wollongong, Australia, July 9-12, 2013.
- [23] Zhong Liang Li, Meng Di Han, and Hai Xia Zhang "A NOVEL MEMS ELECTROMAGNETIC ENERGY HARVESTER WITH SERIES COILS" 978-1-4673-5983-2/13 ©2013 IEEE.
- [24] Tschan, T. and Rooij N.D., Characterisation and modelling of silicon piezoresistive accelerometers fabricated by a bipolar-compatible process. *Sensors and Actuators A*, 1991, pp. 605-609.
- [25] Williams C.B. and Yates R.B, Analysis of a micro-electric generator for microsystems. *Sensors and Actuators A: Physical*, 1996, pp. 8-11.
- [26] Tschan, T. and Rooij N.D., Characterisation and modelling of silicon piezoresistive accelerometers fabricated by a bipolar-compatible process. *Sensors and Actuators A*, 1991, pp. 605-609.
- [27] Pures B. and Lapadatu D., Extremely miniaturized capacitive movement sensors using new suspension systems. *Sensors and Actuators*, 1994, pp. 129-135.
- [28] Strnat K.J., the recent development of permanent magnet materials containing rare earth metals. *IEEE Transaction on magnetics*, 1970, pp. 182-190.
- [29] Arnold, *Soft Magnetics Application Guide-Basics of Magnetics*. The magnetic product group of SPS technologies, 2003
- [30] Blevins R. D., *Formulas for natural frequency and mode shape*, New York : Van Nostrand Reinhold Co.,1979.
- [31] Madou M., *Fundamentals of Microfabrication*. 1997: CRC Press.
- [32] Seidemann V., Butefisch S., and Bttgenbach S., fabrication and investigation of in plane compliant SU-8 structures for MEMS and their application to micro valves and micro grippers. *Sensors and Actuators*, 2002, pp. 457-461.

[33] Moaveni S., Finite element analysis : theory and application with ANSYS. 1999: Upper Saddle River, N.J. : Prentice Hall.